

# "STOP-AND-GO" DECISION-DIRECTED BLIND ADAPTIVE EQUALIZATION USING THE COMPLEX-VALUED MULTILAYER PERCEPTRON

Cheolwoo You and Daesik Hong

Information & Telecommunication Lab., Department of Electronic Engineering,  
Yonsei University, 134 Shinchon-Dong, Seodaemun-Gu, Seoul 120-749 Korea  
Phone: +82-2-361-2871, Fax: +82-2-312-4584, Email: daesikh@catseye.yonsei.ac.kr

## ABSTRACT

In this paper, a "stop-and-go" decision-directed blind equalization scheme is newly proposed. This scheme uses the structure of complex-valued multilayer feedforward neural networks, instead of the linear transversal filters that are usually used in conventional LMS-type blind equalization schemes. A complex-valued activation function composed of two real functions is used. Each real activation function has multi-saturated output region in order to deal with QAM signals of any constellation sizes. Also, the complex backpropagation algorithm is modified for the proposed scheme. Computer simulations are performed to compare the proposed scheme with the conventional "stop-and-go" algorithm in terms of convergence speed, MSE value in the steady state, and constellation of QAM signals after the initial convergence. Simulation results demonstrate the effectiveness of the proposed scheme.

## 1. INTRODUCTION

For blind equalization, many algorithms have been developed. Among useful blind equalization algorithms, there are stochastic-gradient iterative equalization schemes, called LMS-type blind equalization schemes, such as the Sato algorithm [1], the Godard algorithm [2], the "Stop-and-Go" algorithm [3], and so on. These algorithms are based on LMS adaptation, and apply a memoryless nonlinearity in the output of a linear FIR equalization filter for the purpose of generating the "desired response", as shown in Fig. 1. The cost functions of these algorithms are nonconvex functions of the tap weights because of the fact that the estimate, performing the role of an internally generated "desired response", is produced by passing the linear combiner output  $O_p$  through a zero-memory nonlinearity, and also because  $O_p$  is itself a linear function of the tap weights. However, a linear FIR filter structure is not competent to optimize nonconvex functions because the decision regions for a linear machine are convex. Furthermore, if

nonlinear channel distortion is too severe to ignore, these LMS-type blind algorithms suffer from a severe performance degradation because a linear filter with a FIR or lattice structure can only deal with linear channel distortion well. Therefore, a blind equalization scheme using a nonlinear structure has become necessary. On the other hand, Multilayer feedforward neural networks provide a powerful device for approximating a nonlinear input-output mapping of a general nature. Many studies showed that multilayer feedforward neural networks can form convex and nonconvex decision regions because of their nontrivial mapping capabilities [4, 5, 6].

In this paper, a "stop-and-go" decision-directed blind equalization scheme that can deal with QAM signals of any constellation sizes is newly proposed. This scheme uses the structure of complex-valued multilayer feedforward neural networks, instead of the linear transversal filters that are usually used in the conventional LMS-type blind equalization schemes aforementioned. The complex-valued multilayer feedforward neural network works well with M-ary QAM as an equalizer with a training sequence and a CMA-type blind equalizer in recent papers [7, 8]. A complex-valued activation function composed of two real functions is used. Each real activation function has multi-saturated output region adequate to deal with QAM signals of any constellation sizes [7, 8]. In addition, the complex backpropagation algorithm is modified for the proposed scheme.

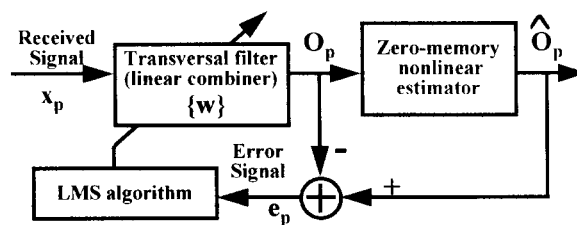


Fig. 1 Block diagram of conventional blind equalizers based on LMS adaptation.

## 2. A COMPLEX ACTIVATION FUNCTION

A complex-valued multilayer perceptron (CMLP) consists of

This work is supported by the Korea Research Foundation  
(# 01-E-0840)

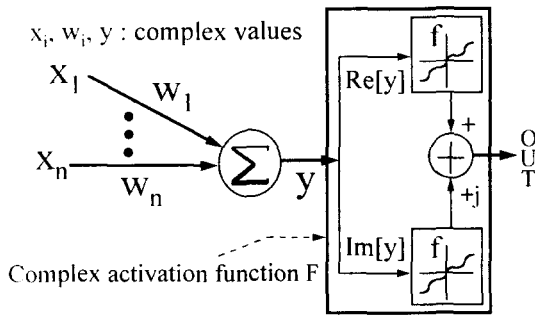


Fig. 2 A single complex processing element (CPE) with a nonlinear activation function.

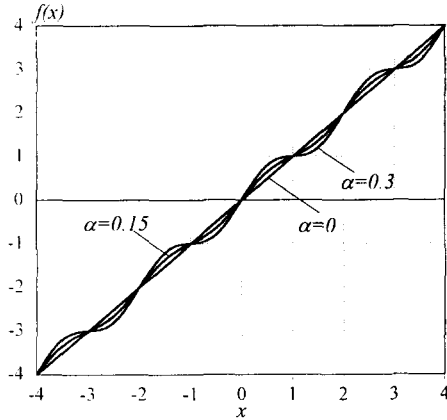


Fig. 3 Input-output characteristic of  $f(x) = x + \alpha \sin(\pi x)$

many complex processing elements (CPE) shown in Fig. 2. The CPE has two real activation functions for the real and the imaginary net values of the node output. The used complex-valued activation function  $F$  is

$$F(y) = f(y_R) + j f(y_I) \quad (1)$$

where " $f$ " is the real-valued function, and " $R$ " and " $I$ " refer to quantities on the real and the imaginary parts, respectively. The real function  $f$  is defined as follows:

$$f(y_{R \text{ or } I}) = y_{R \text{ or } I} + \alpha \sin(\pi y_{R \text{ or } I}) \quad (2)$$

where  $\alpha$  is the *slope* parameter [7, 8]. As shown in Fig. 3,  $f$  has multi-saturated output region adequate to QAM signals of any constellation sizes.

### 3. "STOP-AND-GO" DECISION-DIRECTED ALGORITHM AND ITS NEURAL VERSION

Let  $X_p$  be the complex input vector and  $O_p$  the complex equalizer output [see Fig. 1]. The estimated error is  $\delta_p = \hat{O}_p - O_p$  where  $\hat{O}_p$  is the decided complex symbol. The conventional "stop-and-go" decision-directed (DD) algorithm is as follows:

$$\begin{cases} W_R(p+1) = W_R(p) + \alpha(\zeta_{p,R} \delta_{p,R} X_{p,R} + \zeta_{p,I} \delta_{p,I} X_{p,I}) \\ W_I(p+1) = W_I(p) - \alpha(\zeta_{p,R} \delta_{p,R} X_{p,I} - \zeta_{p,I} \delta_{p,I} X_{p,R}) \end{cases} \quad (3)$$

The above algorithm uses the following flags:

$$\begin{aligned} \zeta_{p,R} &= \begin{cases} 1, & \text{if } \text{sgn } \delta_{p,R} = \text{sgn } \tilde{\delta}_{p,R} \\ 0, & \text{if } \text{sgn } \delta_{p,R} \neq \text{sgn } \tilde{\delta}_{p,R} \end{cases} \\ \zeta_{p,I} &= \begin{cases} 1, & \text{if } \text{sgn } \delta_{p,I} = \text{sgn } \tilde{\delta}_{p,I} \\ 0, & \text{if } \text{sgn } \delta_{p,I} \neq \text{sgn } \tilde{\delta}_{p,I} \end{cases} \end{aligned} \quad (4)$$

where two Sato-like errors

$$\begin{aligned} \tilde{\delta}_{p,R} &= o_{p,R} - (\text{sgn } o_{p,R}) \beta_p \\ \tilde{\delta}_{p,I} &= o_{p,I} - (\text{sgn } o_{p,I}) \beta_p \end{aligned} \quad (5)$$

are used, with  $\beta_p$  being a suitable real value possibly changing with  $p$ .  $\text{sgn}(\cdot)$  is the signum function equal to  $+1$  if the argument is positive, and  $-1$  if it is negative.

On the other hand, if the complex activation function defined by Eqs. (1) and (2), and the CMLP with one output neuron are used, the error terms of the conventional CBP algorithm [7] become as follows:

$$\delta_p = D_p - O_p \quad (6)$$

$$\delta_p^o = f''(net_{p,R}^o) \delta_{p,R} + j f''(net_{p,I}^o) \delta_{p,I} \quad (7)$$

$$\delta_{pi}^h = f'^h(net_{pi,R}^h) (\delta_p^o W_{ji}^{o*})_R + j f'^h(net_{pi,I}^h) (\delta_p^o W_{ji}^{o*})_I \quad (8)$$

where  $W_j^o$  is the weight on the connection from the  $j$ th hidden neuron to the output neuron. In this case, the CBP algorithm may be split into real and imaginary parts as follows:

$$\begin{cases} w_{j,R}^o(p+1) = w_{j,R}^o(p) + \eta (\delta_{p,R}^o i_{pi,R} + \delta_{p,I}^o i_{pi,I}) \\ w_{j,I}^o(p+1) = w_{j,I}^o(p) - \eta (\delta_{p,R}^o i_{pi,I} - \delta_{p,I}^o i_{pi,R}) \end{cases} \quad (9)$$

$$\begin{cases} w_{ji}^h(p+1) = w_{ji}^h(p) + \eta (\delta_{pi,R}^h x_{pi,R} + \delta_{pi,I}^h x_{pi,I}) \\ w_{ji}^h(p+1) = w_{ji}^h(p) - \eta (\delta_{pi,R}^h x_{pi,I} - \delta_{pi,I}^h x_{pi,R}) \end{cases} \quad (10)$$

The "stop-and-go" DD algorithm (S&G) can be naturally extended to blind equalization algorithm using the CMLP. The neural network "stop-and-go" (NNS&G) algorithm is as follows:

$$\begin{cases} w_{j,R}^o(p+1) = w_{j,R}^o(p) + \eta (\zeta_{p,R} \delta_{p,R}^o i_{pi,R} + \zeta_{p,I} \delta_{p,I}^o i_{pi,I}) \\ w_{j,I}^o(p+1) = w_{j,I}^o(p) - \eta (\zeta_{p,R} \delta_{p,R}^o i_{pi,I} - \zeta_{p,I} \delta_{p,I}^o i_{pi,R}) \end{cases} \quad (11)$$

$$\begin{cases} w_{ji}^h(p+1) = w_{ji}^h(p) + \eta (\zeta_{p,R} \delta_{pi,R}^h x_{pi,R} + \zeta_{p,I} \delta_{pi,I}^h x_{pi,I}) \\ w_{ji}^h(p+1) = w_{ji}^h(p) - \eta (\zeta_{p,R} \delta_{pi,R}^h x_{pi,I} - \zeta_{p,I} \delta_{pi,I}^h x_{pi,R}) \end{cases} \quad (12)$$

where  $D_p = \hat{O}_p$  and the same flags defined in Eqs. (4, 5) are used.

#### 4. SIMULATION RESULTS

The performance of the S&G algorithm using the CMLP (NNS&G) is compared with the conventional S&G algorithm (S&G) using the linear FIR filter for 32-QAM signal and 64-QAM signal. The performance is evaluated by calculating the mean square error (MSE). The slope parameter  $\alpha$  is appropriately set through many tests. The reference channel has a relatively flat frequency response. However, its binary eye is closed and the decision-directed attempt to achieve equalizer training was failed. The z-transform notation of the channel is

$$H(z) = (0.0410+j0.0109) + (0.0495+j0.0123)z^{-1} + (0.0672+j0.0170)z^{-2} + (0.0919+j0.0235)z^{-3} + (0.7920+j0.1281)z^{-4} + (0.3960+j0.0871)z^{-5} + (0.2715+j0.0498)z^{-6} + (0.2291+j0.0414)z^{-7} + (0.1287+j0.0154)z^{-8} + (0.1032+j0.0119)z^{-9} \quad (13)$$

In the sequel, we will use the following table notations.

(k)	A linear FIR equalization filter with $k$ tap weights
(N, L)	A CMLP with $N$ input nodes, $L$ hidden neurons and one output neuron
$\mu$	The step-size parameter of a linear FIR filter
$\eta$	The step-size parameter of a CMLP
$[\alpha_1, \alpha_2]$	$\alpha_1$ : The slope parameter of the activation function used for the hidden layer $\alpha_2$ : The slope parameter of the activation function used for the output layer
$w_r$	The reference tap of a linear FIR equalization filter

[\*  $w_{[1+\frac{1}{2}],R}^0$  is always set to one]

As shown in Fig. 4, as the values  $\alpha_1$  and  $\alpha_2$  increase, the convergence speed becomes slow but MSE in the steady state decreases. This is due to the fact that the increased nonlinearity of the activation function accomplishes more powerful mapping capabilities, but causes the learning process to be difficult. For varying the number of input nodes, NNS&G and S&G have shown the similar trend; that is, as the number of tap-weights increases, the convergence speed becomes slow but MSE in the steady state decreases [see Fig. (5)].

The performance comparison between NNS&G and S&G is shown in Fig. 6. As shown in Fig. 6, NNS&G achieves lower MSE in the steady state and the more fast convergence speed than S&G by adjusting the values  $\alpha_1$  and  $\alpha_2$ .

Such results were also observed for 32-QAM signal with  $\beta_p=5$ , as shown in Fig. 7. These are due to the facts that the CMLP has the mapping capability to learn and approximate arbitrary nonlinear functions, and thus can approximate the inverse of the FIR channel more accurately than the linear FIR filter. The powerful mapping capability of NNS&G is more easily observed when the constellation of QAM signals after the initial convergence is plotted. As we can see from Fig. 8, the symbols are more clearly distinguishable at the output of the NNS&G equalizer. Of course, we can see intuitively that such a

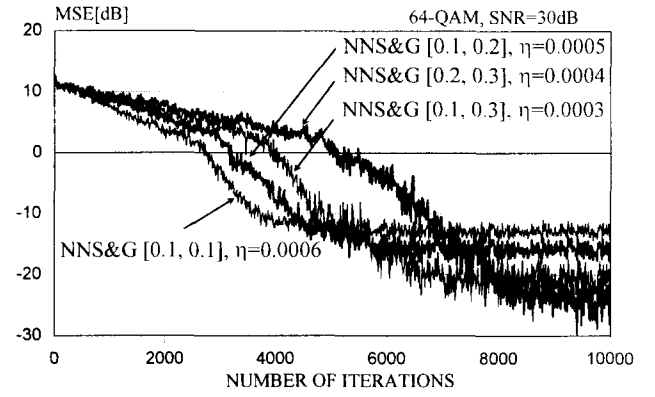
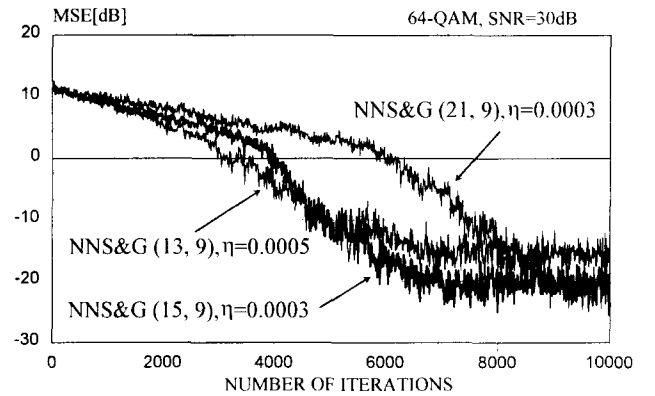
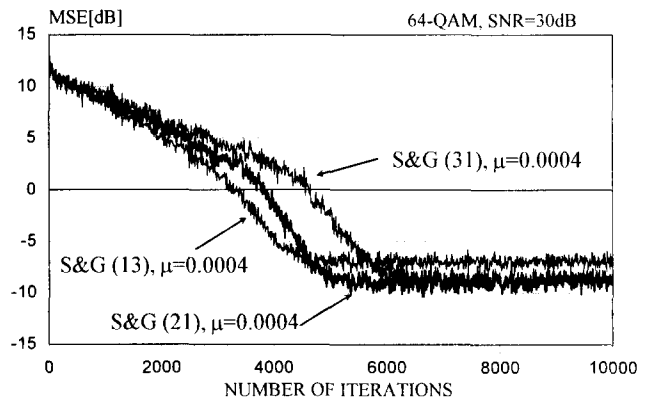


Fig. 4 Convergence of MSE versus number of transmitted symbols for NNS&G (15, 9) with the 64-QAM signal. Parameters are  $\beta_p=6$ ,  $w_{[1+\frac{1}{2}],R}^h=1.0$ .



(a)



(b)

Fig. 5 Convergence of MSE versus number of transmitted 64-QAM symbols for (a) NNS&G [0.1, 0.3] and (b) S&G. Parameters are  $\beta_p=6$ ,  $w_{[1+\frac{1}{2}],R}^h=1.0$ ,  $w_r=1.0$ .

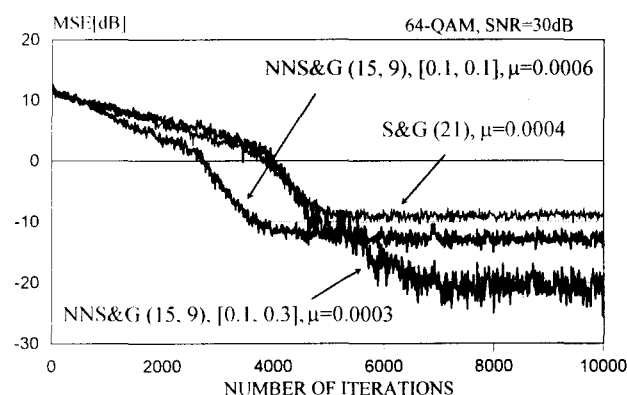


Fig. 6 Convergence of MSE versus number of transmitted 64-QAM symbols.

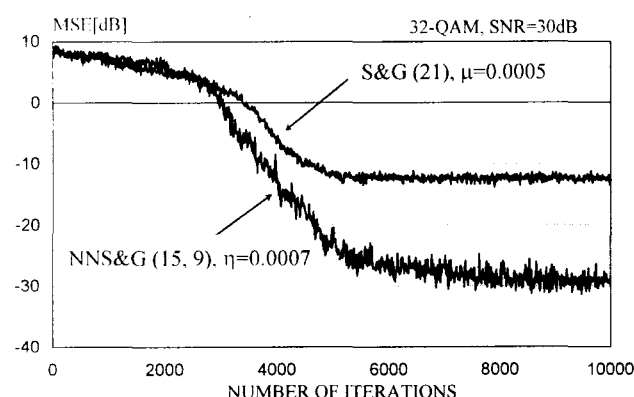


Fig. 7 Convergence of MSE versus number of transmitted 32-QAM symbols for NNS&G [0.1, 0.3] and S&G.

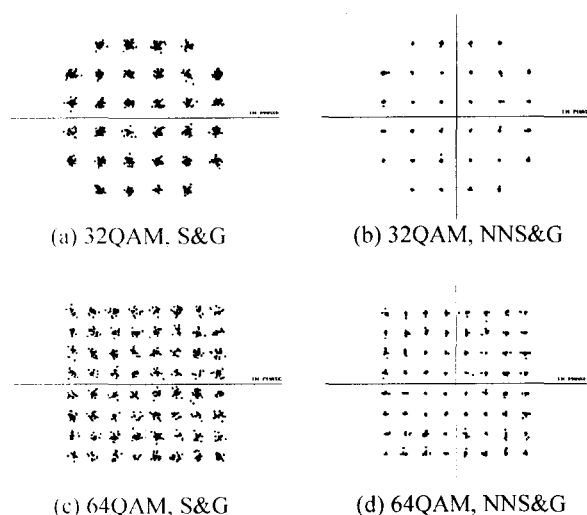


Fig. 8 Constellation of 32- and 64-QAM symbols equalized by S&G and NNS&G.

powerful mapping capability is predominantly generated by the saturation characteristics of the activation function.

## 5. CONCLUSIONS

The "stop-and-go" decision-directed algorithm based on neural networks (NNS&G) has been proposed for M-ary QAM signal of any constellation size. For the proposed scheme, the CMLP with input-memory, being a generalized complex-valued FIR filter, has been used. The CBP algorithm has been modified for the proposed scheme.

Simulation results show that the proposed scheme works well with the 32- and 64-QAM signals as nonlinear blind equalizers. NNS&G achieves much lower MSE in the steady state and more fast convergence speed than S&G for 32-QAM and 64-QAM. However, like the case of S&G, NNS&G's weak point is the initial convergence speed that is relatively slow compared with other LMS-type blind equalization schemes; nevertheless, the robustness to environment conditions such as the step-size parameter and the slope parameters, and the low MSE in the steady state makes NNS&G attractive in contrast to the conventional LMS-type algorithms.

## REFERENCES

- [1] Y. Sato, "A method of self-recovering equalization for multilevel amplitude-modulation systems," *IEEE Trans. on Comm.*, vol. COM-23, pp. 679-682, June 1975.
- [2] D. N. Godard, "Self recovering equalization and carrier tracking in two-dimensional data communication system," *IEEE Trans. on Comm.*, vol. COM-28, pp. 1867-1875, Nov. 1980.
- [3] G. Picchi and G. Prati, "Blind equalization and carrier recovery using a 'stop & go' decision-directed algorithm," *IEEE Trans. on Comm.*, vol. COM-35, pp. 877-887, Sep. 1987.
- [4] M. Arai, "Mapping Abilities of Three-Layer Neural Networks," *Proc. Int'l Joint Conf. on Neural Networks*, Washington D. C., pp. 419-423, June 18-22, 1989.
- [5] J. A. Freemann and D. M. Skapura, *Neural Networks: Algorithms, Applications, and Programming Techniques*, Addison Wesley, 1991.
- [6] J. H. Cho, C. W. You, and D. S. Hong, "The neural decision feedback equalizer for the nonlinear digital magnetic recording channel," *Proc. ICC*, Dallas, pp. 573-576, June 1996.
- [7] C. W. You and D. S. Hong, "Adaptive equalization using the complex backpropagation algorithm," *Proc. IEEE Int'l Conf. on Neural Networks*, Washington D. C., pp. IV 2136-2141, June 2-6, 1996.
- [8] C. W. You and D. S. Hong, "Blind adaptive equalization techniques using the complex multilayer perceptron," *Proc. Globecom96*, London, pp. 1340-1344, Nov. 18-22, 1996.